Molecular Structures and Electronic Transitions of 3,6-Diphenyl-1,2-dithiin and Its Radical Cation: A Spectroelectrochemical and DFT Study

Horst Hennig,*,† Frank Schumer,† Joachim Reinhold,*,‡ Heiner Kaden,§ Wolfram Oelssner,§ Werner Schroth,|| Roland Spitzner,|| and František Hartl*,⊥

Institut für Anorganische Chemie and Wilhelm-Ostwald-Institut für Physikalische und Theoretische Chemie, Universität Leipzig, Johannisallee 29, D-04103 Leipzig, Germany, Kurt-Schwabe-Institut für Mess- und Sensortechnik e.V., D-04720 Ziegra-Knobelsdorf, Germany, Institut für Organische Chemie, Martin-Luther-Universität Halle-Wittenberg Kurt-Mothes-Strasse 2, D 06120 Wittenberg, Germany, and van't Hoff Institute for Molecular Sciences, Universiteit van Amsterdam, Nieuwe Achtergracht 166, 1018 WV Amsterdam, The Netherlands

Received: September 9, 2005; In Final Form: December 4, 2005

One-electron oxidation of 3,6-diphenyl-1,2-dithiin yields the corresponding radical cation. The product is stable at low temperatures and can be distinguished by a triplet EPR signal. Cyclic voltammetric, UV−vis spectroelectrochemical, and DFT studies were performed to elucidate its molecular structure and electronic properties. Time-dependent DFT calculations reproduce appreciably well the UV−vis spectral changes observed during the oxidation. The results reveal a moderately twisted structure of the 1,2-dithiin heterocycle in the radical cation.

Introduction

1,2-Dithiins (1,2-dithiacyclohexadienes), the heterocyclic parent compounds of thiarubrine A and B naturally occurring in plants of the sunflower family *Compositae* (*Asteraceae*),[1] have attracted considerable attention, particularly since they have been synthetically available.[2−4] Because of the biological activity of these compounds, various synthetic investigations have been carried out with the aim of obtaining new classes of antiviral, antifungal, and antibacterial agents containing the pharmacophoric 1,2-dithiin group.[5,6] Furthermore, the explanation of the intense red-to-orange color in the absence of a conventional chromophore and the 8-π-electron anti-aromatic ring system have been interesting subjects of theoretical consideration.[7−9] Particularly interesting are the facile photoinduced extrusion of sulfur to produce thiophenes[10,11] (see Scheme 1) and the electron-transfer behavior giving rise to corresponding dithiolates and radical cations upon (electro)chemical reduction and oxidation, respectively.[7−10,12]

Cyclic voltammetric measurements of 3,6-diphenyl-1,2-dithiin with a twisted conformation (1a, Scheme 1), supported by theoretical studies of 3,6-di-X-1,2-dithiins (X = H, Me), pointed to a geometry change induced by one-electron oxidation, resulting in a flattened 1,2-dithiin ring of the corresponding 3,6-diphenyl-1,2-dithiin radical cation **2a**.[12] On the other hand, the molecular structure and electronic properties of **2a** have not been fully clarified. We have extended the study of the one-electron oxidation of **1a** by means of UV−vis and EPR spectroelectrochemical techniques and time-dependent density functional theory calculations. The data presented in this work describe the anodic process and the nature of the radical cation in more detail, which allows us to modify some of the recently published results.

SCHEME 1

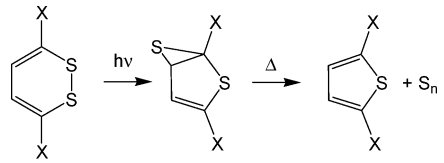

1 **a**: X = Ph
b: X = H
c: X = Me

Experimental Section

General Procedure. All reactions and experiments were conducted under an atmosphere of dry nitrogen or argon, using Schlenk techniques. Solvents were dried by standard procedures and freshly distilled before use.[13] The supporting electrolyte, tetrabutylammonium hexafluorophosphate (Bu_4NPF_6; Aldrich), was recrystallized twice from absolute ethanol and dried overnight at 80 °C under vacuum. Ferrocene (Fc; Schuchardt) and 2,2-diphenyl-1-picrylhydrazyl (DDPH; Aldrich) were used as received. The synthesis of 3,6-diphenyl-1,2-dithiin was performed according to the literature procedure.[2]

Cyclic Voltammetry. Conventional cyclic voltammograms were recorded with a PAAR EG&G model 283 potentiostat, using an airtight, light-protected, single-compartment cell placed in a Faraday cage. The working electrode was a Pt disk (0.42-mm^2 apparent surface area), polished with a 0.25-μm diamond paste between the scans. Coiled Pt and Ag wires served as auxiliary and pseudoreference electrodes, respectively. The concentration of compound **1a** was typically 10^{-3} mol dm^{-3}. Ferrocene (Fc) was used as the internal standard[14] for the determination of electrode potentials and comparison of peak-to-peak potential differences (electrochemical reversibility).

* To whom correspondence should be addressed. Tel.: +49-(0)341-9736160 (H.H), +49-(0)341-9736401 (J.R.), +31-(0)20-5256450 (F.H.). Fax: +49-(0)341-9736199 (H.H), +49-(0)341-9736399 (J.R.), +31-(0)-20-5256456 (F.H.). E-mail: hennigho@chemie.uni-leipzig.de (H.H), reinhold@chemie.uni-leipzig.de (J.R.), f.hartl@uva.nl (F.H.).

† Institut für Anorganische Chemie, Universität Leipzig.

‡ Wilhelm-Ostwald-Institut für Physikalische und Theoretische Chemie, Universität Leipzig.

§ Kurt-Schwabe-Institut für Mess- und Sensortechnik e.V.

|| Martin-Luther-Universität Halle-Wittenberg.

⊥ Universiteit van Amsterdam.

10.1021/jp0551059 CCC: $33.50
Published on Web 01/14/2006

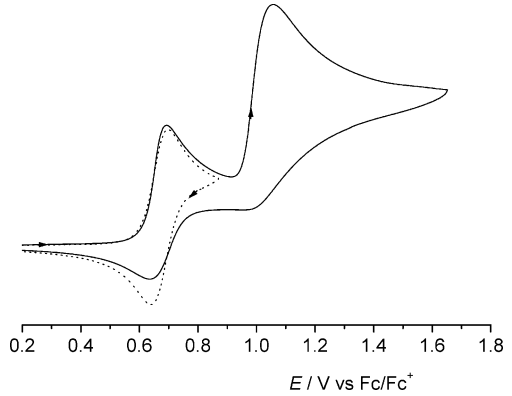

Figure 1. Cyclic voltammogram of 3,6-diphenyl-1,2-dithiin (1a). Conditions: 10^{-3} M **1a** in acetonitrile containing 10^{-1} M $TBAPF_6$, Pt disk working microelectrode ($\nu = 100$ mV s^{-1}, $T = 293$ K).

Conversions of the Fc/Fc^+ potential scale to other reference systems can be found elsewhere.[15]

Spectroelectrochemical Studies. UV−vis spectroelectrochemical experiments at low temperatures were performed with a cryostatted optically transparent thin-layer electrochemical (OTTLE) cell equipped with CaF_2 windows and a Pt minigrid working electrode (32 wires/cm).[16] The rapid electrolysis at room temperature in the time domain of seconds was conducted with another homemade demountable OTTLE cell.[17] The solutions were typically 10^{-1} M in the supporting electrolyte and 10^{-3} M in the analyte.

EPR spectroelectrochemical experiments at low temperatures were carried out with an airtight three-electrode version of the Allendoerfer-type cell equipped with Au-helix working, Pt-helix auxiliary, and Ag-wire pseudoreference electrodes.[18] The solution contained 10^{-3} M **1a** and 3×10^{-1} M supporting electrolyte. The g value was determined against DPPH used as an external standard ($g = 2.0037$).

The working electrode potential of the spectroelectrochemical cells was controlled with a PA4 potentiostat (EKOM, Polna, Czech Republic).

Electronic spectra were recorded in the UV−vis region with software-updated Perkin-Elmer Lambda 5 and Hewlett-Packard 8453 diode-array spectrophotometers and in the NIR region with a Bruker Equinox 55 FT-IR spectrometer equipped with appropriate optics. EPR spectra were obtained with a Varian Century E-104A X-band spectrometer and simulated with the programs PEST WinSIM[19] and Bruker WINEPR SimFonia (version 1.25).

Theoretical Studies. DFT calculations, adopting the widely used B3LYP functionals,[20,21] were carried out using the Gaussian 03 program package.[22] The 6-31g(d) basis set[23] was used throughout the investigations. Comparative calculations with the 6-31g(d,p) and 6-311g(d) basis sets only slightly changed the obtained parameters, but did not modify any of the qualitative conclusions. The stationary points resulting from the optimizations were characterized by frequency analysis. The influence of a model solvent (acetonitrile) was checked with the COSMO continuum model[24,25] (conductor-like screening model). The electronic transitions in **1a** and **2a** were determined by applying the time-dependent DFT procedure.

Results and Discussion

Electrochemistry of 3,6-Diphenyl-1,2-dithiin (1a). *Cyclic Voltammetry.* The cyclic voltammogram of parent **1a** in butyronitrile recorded at 293 K (Figure 1) shows two oxidations at $E_{1/2} = 0.67$ V and $E_{p,a} = 1.02$ V vs Fc/Fc^+. The first anodic step belongs to one-electron oxidation yielding the corresponding 1,2-dithiin radical cation (**2a**). The peak-to-peak separation, ΔE_p, for this redox couple (89 mV) slightly exceeds the value for the ferrocene/ferrocenium (Fc/Fc^+) internal standard (79 mV) at moderate scan rates (100 mV s^{-1}). The cathodic-to-anodic peak-current ratio, i_c/i_a, is less than unity in this time domain, increasing from 0.90 at 100 mV s^{-1} to 0.94 at 1 V s^{-1}. The second anodic step is totally irreversible at room temperature and was not investigated in detail. This cyclic voltammetric response of **1a** is essentially the same as that obtained in acetonitrile by Block et al.,[12] who fitted the first anodic process to an EC mechanism and determined the rate constant for the following chemical reaction, $k_f = 0.318$ s^{-1}. The chemical step was associated with a conformational change from the twisted structure of **1a** to the flattened form of one-electron-oxidized **2a** (see Scheme 2).[12] However, no attention was paid to the thermal decomposition of **2a**, such as disproportionation reported[9] for the radical cation of 1,2-dithiin annelated with bicyclo[2.2.2]octane, as an alternative chemical process in the EC mechanism. We probed the thermal stability of **2a** by UV−vis spectroelectrochemistry.

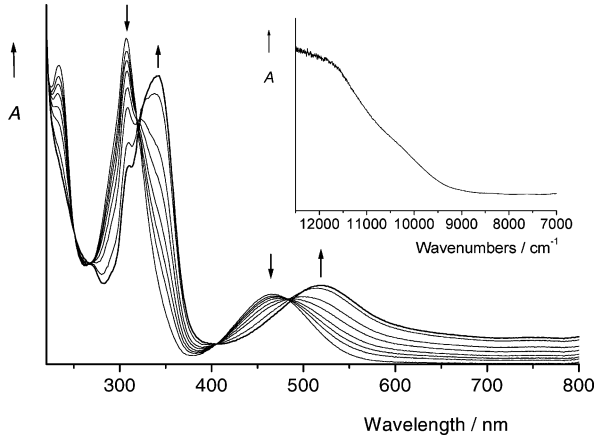

Figure 2. UV−vis spectral changes accompanying the controlled-potential oxidation of 3,6-diphenyl-1,2-dithiin (**1a**) to corresponding radical cation **2a** within a low-temperature OTTLE cell.[16] Conditons: butyronitrile, 223 K. Inset: Electronic spectrum of **2a** in the NIR spectral region.

SCHEME 2

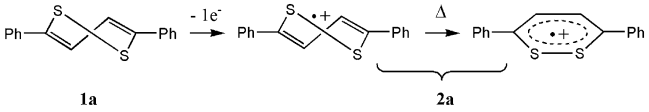

UV−Vis Spectroelectrochemistry. To avoid thermal decomposition, the oxidation of **1a** was performed in butyronitrile at 223 K, using a cryostated optically transparent thin-layer electrochemical (OTTLE) cell.[16] The corresponding UV−vis spectral changes are depicted in Figure 2. The spectra show the smooth conversion of the parent compound **1a** absorbing at 308 nm (corresponding to an excitation energy of 32500 cm^{-1}) and 465 nm (21500 cm^{-1}) to the radical cation **2a** absorbing at 330 nm (30300 cm^{-1}) and 520 nm (19200 cm^{-1}). The presence of several isobestic points confirms the stability of **2a**. Additional new unresolved absorption in the low-energy region (600−1100 nm; Figure 2, inset) is also characteristic of **2a**, as documented in the DFT section below.

At 293 K, the UV−vis spectroelectrochemical experiment resulted in strongly diminished absorption in the visible region; the only remaining feature was a weak absorption band at about 485 nm. The visible absorption due to one-electron-oxidized

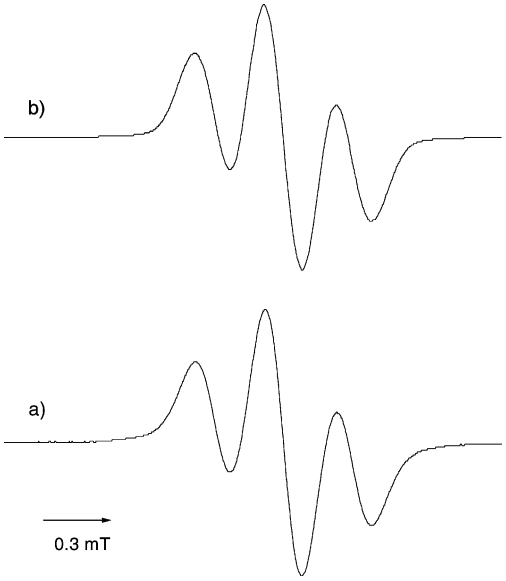

Figure 3. (a) EPR spectrum of the radical cation of 3,6-diphenyl-1,2-dithiin (**2a**) recorded in situ using a thin-layer spectroelectrochemical cell.[18] Conditions: 10^{-3} M **1a** oxidized by controlled-potential electrolysis in dichloromethane at 223 K. (b) Simulated spectrum.

2a was observable at room temperature merely for a few seconds upon diode-array detection, when oxidizing parent **1a** within the OTTLE cell in a potential-step fashion. Clearly, radical cation **2a** is not sufficiently stable to be obtained at room temperature.

EPR Spectroelectrochemistry. The radical nature of **2a** was confirmed by EPR spectroscopy. Similarly to the UV−vis spectroelectrochemical investigation, the oxidation of **1a** was carried out in dichloromethane at 223 K within a coaxial three-electrode cell.[18] The reversibility of the anodic process was checked by thin-layer cyclic voltammograms recorded at $\upsilon = 2$ mV s^{-1} before and after each EPR measurement. Electrolysis at the applied anodic peak potential of **1a** led to the appearance of a well-resolved triplet signal at $g = 2.0095$ (Figure 3). The hyperfine splitting can be attributed to the two magnetically equivalent ^{1}H nuclei in positions 4 and 5 of the central 1,2-dithiin ring: $a_H = 0.34$ mT. At sufficiently high amplification, the EPR spectrum of **2a** showed symmetrical satellites assigned to the ^{33}S ($I = {}^3/_2$, 0.75% natural abundance) hyperfine splitting. Spectral simulation revealed partly hidden nine satellite lines with a 1:2(7×):1 pattern, arising from the presence of one ^{33}S nucleus in the 1,2-dithiin heterocycle: $a_S = 0.70$ mT. The very weak 15-line signal of **2a** containing two ^{33}S nuclei in natural abundance was not resolved in the spectral noise. The experimental a_H and a_S values resemble the situation in the radical cation of 1,8-dithianaphthalene with high spin density at the sulfur atoms.[26] It is also noteworthy that the radical cation of the annelated 1,2-dithiin reported[9] by Komatsu et al. shows an EPR signal with a resolved hyperfine structure at same magnetic field position: $g = 2.0095$.

It should be recalled that Block et al.[12] observed at room temperature an EPR signal of a radical species formed by oxidation of **1a** with anhydrous $AlCl_3$ in CH_2Cl_2. The signal was assigned to the radical cation of parent **1a**, i.e., the one-electron oxidation product observable with cyclic voltammetry at moderate scan rates. However, the EPR spectrum was not identical to our observation and exhibited an unresolved broad singlet at a different field position ($g = 2.0019$). No attempts were made to check the identity of the chemically oxidized radical species.

Figure 4. Optimized structure of 3,6-diphenyl-1,2-dithiin radical cation 2a.

TABLE 1. Results of the DFT Optimizations of Selected Neutral 3,6-Di-X-1,2-dithiins and the Corresponding Radical Cations[a]

	X = Ph		X = H		X = Me	
Neutral Molecules	**1a**	**1ap**	**1b**	**1bp**	**1c**	**1cp**
S−S	209.7	216.4	210.9	217.0	210.0	215.8
C−S−S−C	52	0	49	0	51	0
H−C−C−H	25	0	24	0	24	0
(H−)C−C−C−C(−H)	32	42				
ΔE		35		21		23

Radical Cations	**2a**	**2ap**	**2b**	**2c**
S−S	210.3	211.5	210.3	210.0
C−S−S−C	31	0	0	0
H−C−C−H	11	0	0	0
(H−)C−C−C−C(−H)	31	38		
ΔE		10		

[a] Selected structural parameters (pm and deg) and destabilization of a model structure with planar heterocycle with regard to the twisted minimum structure (kJ mol^{-1}). The symbol p applies for hypothetical structures with forced planarity (**1ap**, **1bp**, **1cp**, and **2ap**); these structures are saddle points. For **2b** and **2c**, the planarity followed from the optimizations; these are the minimum structures.

DFT Calculations. *Molecular and Electronic Structures*. To provide information concerning the hitherto unknown molecular structure of radical cation **2a**, geometry optimizations were performed. Using standard DFT techniques, a C_2-symmetric minimum structure results (Figure 4). Selected structural parameters are given in Table 1. The most striking feature is the twisting of the central 1,2-dithiin heterocycle with a moderate torsion angle (31°) for the C−S−S−C unit and a small angle (11°) for H−C−C−H. The phenyl substituents are, as expected, twisted with regard to the 1,2-dithiin ring, with a (H−)C−C−C−C(−H) torsion angle of 31°. These values change only slightly, within a few degrees, when the basis set is varied (for computational details, see the Experimental Section).

Table 1 also contains the results obtained for the neutral 3,6-diphenyl-1,2-dithiin molecule (**1a**). Moreover, to contribute to the investigation of the structural and electronic properties of the whole class of 3,6-disubstituted 1,2-dithiins, the nonsubstituted compounds, **1b** and **2b**, and the dimethyl derivatives, **1c** and **2c**, were also included in the calculations. Selected structural and energetic parameters resulting from the optimizations are collected in Table 1.

For the neutral systems, the minimum structure is, in each case, a strongly twisted one (C_2 symmetry), with a C−S−S−C torsion angle of around 50°, in good agreement with the crystal structure of **1a** (59.0°)[27] as well as with the structural data for the nonsubstituted 1,2-dithiin (**1b**) obtained from microwave spectroscopy (53.9°)[28] and from various geometry optimizations.[7−9,12] The calculated S−S bond length is, in each case, somewhat larger than the experimental data, again in agreement with other experiences.[9] To gain information concerning the amount of stabilization due to the twisting of the 1,2-dithiin ring (to be discussed hereinafter), hypothetical structures were optimized, for which the 1,2-dithiin ring was forced to be planar. The resulting structures, **1bp** and **1cp** (both with C_{2v} symmetry), are calculated to lie 21 and 23 kJ mol^{-1}, respectively, above

the minimum structure. For **1ap** (C_2 symmetry), the corresponding energetic position is somewhat higher (35 kJ mol^{-1}).

For the radical cations, the picture is less uniform. For both the nonsubstituted radical cation, **2b**, and the dimethyl-substituted one, **2c**, the DFT optimizations, starting from a twisted structure, flatten the 1,2-dithiin unit, resulting in a minimum structure with a planar ring (C_{2v} symmetry). This has also been found by Komatsu et al. for the radical cation of the annelated 1,2-dithiin.[9] We remark that other authors,[12] using MP2 optimizations, obtained very little twisting for **1b** and **2b** (with C−S−S−C torsion angles of 6.3° and 14.2°, respectively). It follows that, for the latter systems, the potential curve concerning the ring twisting is very flat. However, for the radical cation of 3,6-diphenyl-1,2-dithiin, **2a**, the system in which we are mainly interested, a distinct 1,2-dithiin twisting results as described above (cf. Figure 4). The hypothetical structure with the planar 1,2-dithiin ring, **2ap**, is calculated to lie 10 kJ mol^{-1} higher in energy.

This energy difference corresponds to the gas-phase situation. To examine the influence of a solvent on the gas-phase parameters, optimizations were performed with a model solvent (acetonitrile), applying the COSMO continuum model (for details, see the Experimental Section). It follows, as could be expected for the rather apolar systems under study, that only minor changes of the structural and energetic parameters result. Actually, the energy difference between structures **2a** and **2ap** is reduced to 8 kJ mol^{-1}.

To rationalize the energetic reasons for the different twisting in **1a** and **2a** and to provide basic information for the assignment of the electronic transitions in these species (see below), the frontier orbital pictures and energies are schematically depicted in Figure 5.

A recent discussion of the frontier orbital structure of **1b** was based on the interaction of butadiene and disulfide fragments.[8] As a different starting point, we look at the well-known π-orbital structure of a planar six-membered polyene ring (Figure 6). Introducing two heteroatoms in the ortho positions (the two positions at the ring bottom in the figure) reduces the symmetry from D_{6h} to C_{2v}, i.e., the degenerate orbital pairs split. We compare Figure 6 with the frontier orbital structure resulting for the model system with the planar heterocycle (**1ap**) displayed in Figure 5a (having C_2 symmetry because of the orientation of the phenyl groups). The eight π electrons of the 1,2-dithiin moiety reside in two b and two a orbitals, the latter being the highest occupied orbitals of **1ap**. It appears that the HOMO and HOMO − 1 have very similar characters, showing relatively strong π-antibonding contributions from the two sulfur atoms. The LUMO corresponds to the second orbital of the initially degenerate π^* orbital pair of the polyene ring. It has a weak S−S π-bonding contribution, being mainly delocalized within the butadiene-like fragment. The LUMO + 1 is a S−S σ-antibonding orbital.

Compared to the aromatic 6-π-electron system, the additional occupation of a S−S antibonding orbital in the 1,2-dithiin system destabilizes the planar heterocycle. This should result in a certain twisting. In fact, because of the twisting of the ring, the HOMO and HOMO − 1 lose some of their S−S π-antibonding character and gain some S−S σ-bonding character, leading to a stabilization of the resulting a-symmetry orbitals. This is visualized in Figure 5b presenting the frontier orbital structure obtained for the neutral 1,2-dithiin system **1a**. It appears that the orbital stabilization with regard to **1ap** is more distinct for the HOMO than for the HOMO − 1. This reflects that the occupation of the HOMO in the 8-π-electron system is responsible for the

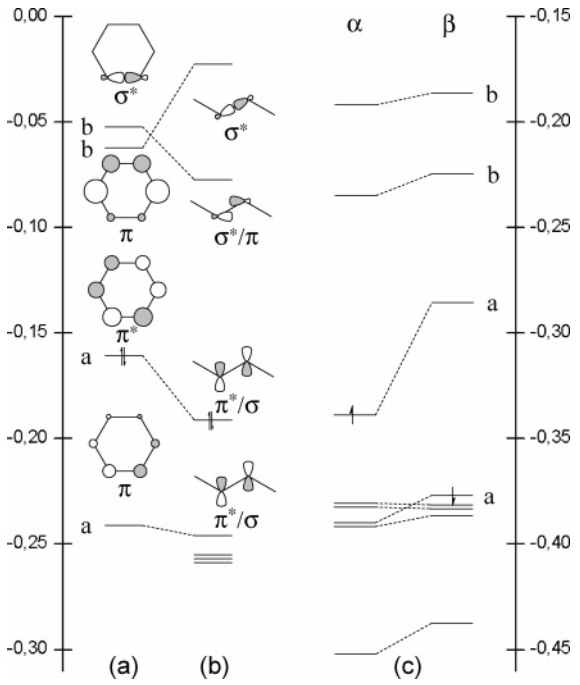

Figure 5. Frontier molecular orbitals and energies (eV) of 3,6-diphenyl-1,2-dithiin (a) in the model structure **1ap** with planar 1,2-dithiin heterocycle and (b) in the twisted minimum structure **1a** (here, only the S−S bonding/antibonding contributions are indicated), as well as (c) in radical cation **2a**. In each case, the occupation is indicated only for the highest occupied orbital. The orbital characteristics for **2a** correspond to those depicted for **1a**. For **2a**, in addition to the frontier orbitals localized at the 1,2-dithiin ring, three spin−orbital pairs of similar energy originating from the phenyl rings are relevant. An S−S π-bonding orbital pair of the 1,2-dithiin ring follows in decreasing energy.

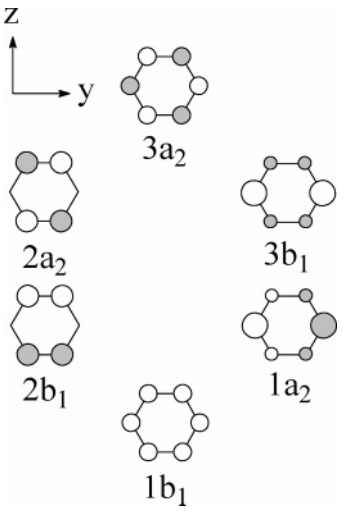

Figure 6. π-orbital structure of a planar six-membered ring with symmetry characterization regarding to the reduced symmetry (C_{2v}).

ring destabilization. Consequently, the total energy and the S−S bond distance should decrease upon twisting. In fact, the neutral 1,2-dithiin systems, with the doubly occupied HOMO, are strongly twisted, which is paired with a significant decrease of the total energy and the S−S bond distance compared to the model systems with planar heterocycles (see Table 1). This situation is independent of any substituents in the 3 and 6 positions.

For the radical cations, the situation is more complex. The DFT optimizations of **2b** and **2c** resulted in planar structures. Obviously, in these cases, occupation of the HOMO with only

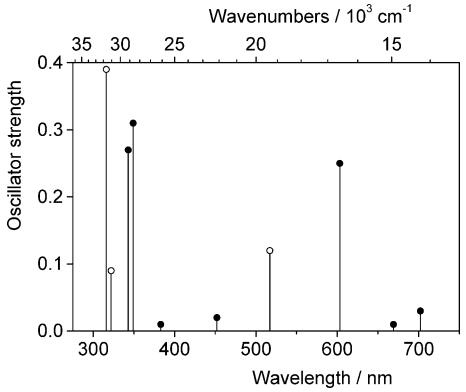

Figure 7. Calculated electronic excitations (energies and oscillator strengths *f*) for 3,6-diphenyl-1,2-dithiin **1a** (○) and its radical cation **2a** (●) to be compared with the experimental UV−vis spectra of **1a** and **2a** shown in Figure 2.

one electron does not induce any noticeable destabilizing effect to be reduced by twisting. Keeping in mind that Komatsu et al. also found a planar 1,2-dithiin ring for the radical cation of the annelated 1,2-dithiin,[9] it can be concluded that the moderate twisting of the heterocycle obtained for the radical cation of 3,6-diphenyl-1,2-dithiin (**2a**) is basically caused by the peculiarities of the phenyl substituents. A comparison of the torsion angle between the phenyl substituents and the planar 1,2-dithiin ring in **2ap** (38°) with the torsion angle in biphenyl, for which we obtained a value of 39° when applying the same computational procedure, points to the same origin of twisting, i.e., avoiding a strong repulsion between neighbored hydrogens. In such a twisted system with C_2 symmetry (**2ap**), the planarity of the central unit is a model constraint. Actually, there is no need for the slightly destabilized 1,2-dithiin ring to remain strictly planar. Thus, we conclude that the moderate twisting of the heterocycle in **2a** is not fundamentally caused by the intrinsic electronic properties of the 7-π-electron system of the 1,2-dithiin ring. Rather, it might be a consequence of the twisting of the phenyl groups with respect to the central unit.

The calculation of the hyperfine coupling constant a_H for the radical cation **2a** resulted in a value of −0.32 mT, in good agreement with the measured value of 0.34 mT (see above). The negative sign corresponds to the negative sign of the spin density (−0.0060) obtained for the hydrogen atoms at the 4 and 5 positions of the 1,2-dithiin ring. It indicates that the spin density is dominated by an effective spin polarization in the formally doubly occupied orbitals. The (positive) contribution of the singly occupied orbital (SOMO) to the spin density at the hydrogen atoms is, as expected, unimportant, because this orbital has essentially a π character (in line with the orbital characteristic of the HOMO given in Figure 5). These relations are confirmed by the respective values resulting for **2ap** (hydrogen spin density = −0.0068, a_H = −0.38 mT). In the latter system, with a planar dithiin ring, the SOMO is an almost perfect π orbital with further reduced (positive) hydrogen contributions.

Calculation of Electronic Transitions. To interpret the UV−vis spectral changes observed during the in situ oxidation of 1a to **2a** (Figure 2), we performed time-dependent DFT calculations. Adopting the optimized molecular structures, the excited singlet states were determined up to excitation energies of ca. 33000 cm^{-1}, giving rise to absorption maxima above 300 nm. The calculated excitation energies and intensities (indicated by the oscillator strength *f*) are given in Table 2.

It turns out that the dominating excitations are directed to the LUMO and LUMO + 1. Therefore, we also must consider

TABLE 2. Electronic Transitions in 1a and 2a Resulting from Time-Dependent DFT Calculations

compd	excitation energy (10^3 cm^{-1})	wavelength (nm)	oscillator strength *f*	dominating excitations	S−S bonding character
1a					
1	19.3	517	0.12	HOMO → LUMO	$\pi^*/\sigma \rightarrow \sigma^*/\pi$
2	31.0	322	0.09	HOMO − 1 → LUMO	$\pi^*/\sigma \rightarrow \sigma^*/\pi$
3	31.6	316	0.39	HOMO → LUMO + 1	$\pi^*/\sigma \rightarrow \sigma^*$
2a					
1	14.2	702	0.03	α HOMO → α LUMO	$\pi^*/\sigma \rightarrow \sigma^*/\pi$
3	14.9	669	0.01	β HOMO → β LUMO	$\pi^*/\sigma \rightarrow \pi^*/\sigma$
5	16.5	603	0.25	β HOMO − 3 → β LUMO	phenyl $\pi \rightarrow \pi^*/\sigma$
6	22.1	452	0.02	α HOMO → α LUMO + 1	$\pi^*/\sigma \rightarrow \sigma^*$
11	26.0	383	0.01	β HOMO − 4 → β LUMO	$\pi/\sigma^* \rightarrow \pi^*/\sigma$
13	28.6	349	0.31	α HOMO − 3 → α LUMO	$\pi^*/\sigma \rightarrow \sigma^*/\pi$
				β HOMO → β LUMO + 1	$\pi^*/\sigma \rightarrow \sigma^*/\pi$
14	29.1	343	0.27	β HOMO − 1 → β LUMO + 1	phenyl $\pi \rightarrow \sigma^*/\pi$

what happens with the characters of the two empty orbitals because of the twisting (see Figure 5a,b). Both orbitals are of b symmetry in C_2. Thus, upon twisting, they will mix to a certain amount, resulting in two orbitals with similar characters. Considering, in more detail, the atomic contributions to the two lowest unoccupied orbitals, as they result from the calculations, it turns out that both orbitals have, in particular, large sulfur contributions. The LUMO of 1a does not contain any contribution from the sulfur p_π orbitals. Thus, we consider this orbital to correspond essentially to the LUMO + 1 of **1ap**. Upon twisting, this orbital becomes stabilized by losing some of its S−S σ-antibonding character and gaining some S−S π-bonding character. The small involvement of sulfur p_π orbitals in the LUMO of **1ap** can be found in the LUMO + 1 of **1a**, which, moreover, gains remarkable S−S σ-antibonding contributions. In the twisted geometry, this orbital is effectively S−S σ antibonding and, hence, strongly destabilized.

The electronic absorption spectrum of 3,6-diphenyl-1,2-dithiin (**1a**) is considered first. The calculated excitations are visualized in Figure 7. Comparing these results with the experimental UV−vis−NIR spectrum shown in Figure 2, it appears that the calculated lowest-energy transition of medium intensity at 19300 cm^{-1} (517 nm) reproduces fairly well the measured absorption maximum at 21500 cm^{-1} (465 nm). It is assigned to the HOMO → LUMO transition having a $\pi^*/\sigma \rightarrow \sigma^*/\pi$ character with regard to the S−S bonding properties. This transition is responsible for the red color of the system, as has also been concluded for other 1,2-dithiin systems.[8] An intense UV transition calculated at 31600 cm^{-1} (316 nm) fits perfectly the measured absorption maximum at 32500 cm^{-1} (308 nm). It is assigned to a HOMO → LUMO + 1 excitation with a $\pi^*/\sigma \rightarrow \sigma^*$ character. Finally, a low-intensity transition resulted at 31000 cm^{-1} (322 nm), which corresponds to a HOMO − 1 → LUMO excitation having a $\pi^*/\sigma \rightarrow \sigma^*/\pi$ character; it should be responsible for the asymmetric shape of the high-intensity UV absorption band of **1a**.

The frontier orbital energies of radical cation **2a**, obtained for the optimized structure, are given in Figure 5c. Because of the unrestricted computational scheme, the orbital pairs split. The α orbitals are stabilized compared to the β orbitals

(assuming that the "unpaired" electron bears α spin). The symmetry and the bonding character of these spin−orbital pairs correspond to those depicted for the doubly occupied orbital pairs of **1a** (Figure 5b). In addition to the frontier orbitals localized at the 1,2-dithiin moiety, several phenyl π orbitals become relevant. The splitting of the corresponding spin−orbital pairs is unimportant, because the contribution of the phenyl rings to the SOMO is very small. Finally, the highest S−S π-bonding orbital turns out to be involved in the excitations.

The calculated medium-intensity transition at 16500 cm^{-1} (603 nm) is red-shifted by 2700 cm^{-1} compared to the 520-nm absorption maximum in the experimental spectrum of 2a, and by 2800 cm^{-1} from the calculated lowest-energy transition of **1a**. The latter difference is in good agreement with the measured shift (2300 cm^{-1}). Furthermore, the increased intensity of the main visible absorption on oxidation of **1a** to **2a** is correctly reproduced. At first glance, this transition of **2a** should correspond, in analogy to **1a**, to the α HOMO → α LUMO excitation. The calculations show, however, that the situation is quite different. An excitation from a phenyl π orbital to the β LUMO (or, in terms of a restricted scheme, to the SOMO) appears to be responsible for the color of radical cation **2a**. The lowest-energy excitation (α HOMO → α LUMO) of **2a** is calculated to be at 14200 cm^{-1} (702 nm), having a very low intensity. In the region between 700 and 600 nm, we obtain several other excitations, also with low intensities. Those with $f < 0.01$ are not included in Table 2 and Figure 7. All of them are assigned as excitations to the β LUMO (SOMO). This explains why the unresolved absorption at longer wavelengths appears only for radical cation **2a**, but not for the neutral molecule **1a**. Finally, the high-intensity UV transition of **2a** can be associated with two neighboring excitations calculated at 28600 cm^{-1} (349 nm) and 29100 cm^{-1} (343 nm), with a mean red shift of 2700 cm^{-1} with respect to the high-intensity transition of **1a**. This agrees reasonably with the experimental shift of 2300 cm^{-1} and the broader absorption band. One of these excitations is essentially located at the disulfide fragment and thus corresponds to the high-intensity transition of **1a**. The other one originates in the π system of the phenyl substituents.

Conclusions

The electron-transfer behavior of 3,6-diphenyl-1,2-dithiin (**1a**) was studied by UV−vis and EPR spectroelectrochemical methods. The one-electron oxidation of **1a** at low temperatures leads to the stable radical cation (**2a**). To provide information concerning the hitherto unknown molecular structure of **2a**, geometry optimizations were performed for this and several related systems. The results point to a moderately twisted structure of the 1,2-dithiin heterocycle in **2a**. Time-dependent DFT calculations reproduce appreciably well the UV−vis spectral changes observed during the oxidation of **1a** to **2a**, in line with a literature review on sulfur-containing organic chromophores.[29] Consequently, the assignments of the experimentally recorded absorption bands of **1a** and **2a** should be reasonable.

The conformational change caused by the one-electron oxidation of 1a is most likely faster than anticipated in the literature.[12,30] The chemical step in the EC mechanism (k_f = 0.318 s^{-1}) of the anodic process is ascribed to the thermal instability of radical cation **2a**.

Acknowledgment. Financial support of parts of this work by the Freistaat Sachsen is highly appreciated. The electronic spectra in the NIR region were recorded in the laboratory of Professor Saverio Santi (University of Padova, Padova, Italy).

References and Notes

(1) Bohlmann, F.; Kleine, K.-M. *Chem. Ber.* **1965**, *98*, 3081−3086.
(2) Schroth, W.; Billig, F.; Reinhold: G. *Angew. Chem., Int. Ed. Engl.* **1967**, *6*, 689−699
(3) Block, E.; Guo, C.; Thiruvazhi, M.; Toscano, P. J. *J. Am. Chem. Soc.* **1994**, *116*, 9403−9404.
(4) Koreeda, M.; Yang, W. *J. Am. Chem. Soc.* **1994**, *116*, 10793−10794.
(5) Page, J.; Block, E.; Towers, G. H. N. *Photochem. Photobiol.* **1999**, *70*, 159−165.
(6) Bierer, D. E.; Dener, J. M.; Dubenko, L. G.; Gerber, R. E.; Litvak, J.; Peterli, S.; Peterli-Roth, P.; Truong, T. V.; Mao, G.; Bauer, B. E. *J. Med. Chem.* **1995**, *38*, 2628−2648.
(7) (a) Mann, M.; Fabian, J. *J. Mol. Struct. (THEOCHEM)* **1995**, *331*, 51−61. (b) Fabian, J.; Mann, M.; Petiau, M. *J. Mol. Model.* **2000**, *6*, 177−185.
(8) Glass, R. S.; Gruhn, N. E.; Lichtenberger, D. L.; Lorance, E.; Pollard, J. R.; Birringer, M.; Block, E.; DeOrazio, R.; He, C.; Shan, Z.; Zhang, X. *J. Am. Chem. Soc.* **2000**, *122*, 5065−5074.
(9) Wakamiya, A.; Nishinaga, T.; Komatsu, K. *J. Am. Chem. Soc.* **2002**, *124*, 15038−15050.
(10) Schroth, W.; Hintzsche, E.; Spitzner, R.; Ströhl, D.; Sieler, J. *Tetrahedron* **1995**, *51*, 13247−13260.
(11) Block, E.; Page, J.; Toscano, P. J.; Wang, C. X.; Zhang, X.; DeOrazio, R.; Guo, C.; Sheridan, R. S.; Towers, G. H. N. *J. Am. Chem. Soc.* **1996**, *118*, 4719−4720.
(12) Block, E.; Birringer, M.; DeOrazio, R.; Fabian, J.; Glass, R. S.; Guo, C.; He, C.; Lorance, E.; Quian, Q.; Schroeder, T. B.; Shan, Z.; Thiruvazhi, M.; Wilson, G. S.; Zhang, X. *J. Am. Chem. Soc.* **2000**, *122*, 5052−5064.
(13) Perrin, D. D.; Armarego, W. F. L. In *Purification of Laboratory Chemicals*, 3rd ed.; Pergamon Press: New York, 1988.
(14) Gritzner, G.; Kùta, J. *Pure Appl. Chem.* **1984**, *56*, 462−466.
(15) Pavlishchuk, V. V.; Addison, A. W. *Inorg. Chim. Acta* **2000**, *298*, 97−102.
(16) (a) Hartl, F.; Luyten, H.; Nieuwenhuis, H. A.; Schoemaker, G. C. *Appl. Spectrosc.* **1994**, *48*, 1522−1528. (b) Mahabiersing, T.; Luyten, H.; Nieuwendam, R. C.; Hartl, F. *Collect. Czech. Chem. Commun.* **2003**, *68*, 1687−1709.
(17) Krejčík, M.; Daněk, M.; Hartl, F. *J. Electroanal. Chem.* **1991**, *317*, 179−187.
(18) Hartl, F.; Groenestein; R. P.; Mahabiersing, T. *Collect. Czech. Chem. Commun.* **2001**, *66*, 52−66.
(19) Public EPR Software Tools, National Institute of Environmental Health Sciences, available at http://epr.niehs.nih.gov/pest.html (accessed September 2002). References listed in the PEST manual reference section.
(20) Becke, A. D. *J. Chem. Phys.* **1993**, *98*, 5648−5652.
(21) Lee, C.; Yang, W.; Parr, R. G. *Phys. Rev. B* **1988**, *37*, 785−789.
(22) Frisch, M. J.; Trucks, G. W.; Schlegel, H. B.; Scuseria, G. E.; Robb, M. A.; Cheeseman, J. R.; Montgomery, J. A., Jr.; Vreven, T.; Kudin, K. N.; Burant, J. C.; Millam, J. M.; Iyengar, S. S.; Tomasi, J.; Barone, V.; Mennucci, B.; Cossi, M.; Scalmani, G.; Rega, N.; Petersson, G. A.; Nakatsuji, H.; Hada, M.; Ehara, M.; Toyota, K.; Fukuda, R.; Hasegawa, J.; Ishida, M.; Nakajima, T.; Honda, Y.; Kitao, O.; Nakai, H.; Klene, M.; Li, X.; Knox, J. E.; Hratchian, H. P.; Cross, J. B.; Adamo, C.; Jaramillo, J.; Gomperts, R.; Stratmann, R. E.; Yazyev, O.; Austin, A. J.; Cammi, R.; Pomelli, C.; Ochterski, J. W.; Ayala, P. Y.; Morokuma, K.; Voth, G. A.; Salvador, P.; Dannenberg, J. J.; Zakrzewski, V. G.; Dapprich, S.; Daniels, A. D.; Strain, M. C.; Farkas, O.; Malick, D. K.; Rabuck, A. D.; Raghavachari, K.; Foresman, J. B.; Ortiz, J. V.; Cui, Q.; Baboul, A. G.; Clifford, S.; Cioslowski, J.; Stefanov, B. B.; Liu, G.; Liashenko, A.; Piskorz, P.; Komaromi, I.; Martin, R. L.; Fox, D. J.; Keith, T.; Al-Laham, M. A.; Peng, C. Y.; Nanayakkara, A.; Challacombe, M.; Gill, P. M. W.; Johnson, B.; Chen, W.; Wong, M. W.; Gonzalez, C.; Pople, J. A. *Gaussian 03*, revision B.03; Gaussian, Inc.: Pittsburgh, PA, 2003.
(23) Hehre, W. J.; Radom, L. v. R.; Schleyer, P.; Pople, J. In *Ab Initio Molecular Orbital Theory*; Wiley: New York, 1986.
(24) Klamt, A.; Schüürmann, G. *J. Chem. Soc., Perkin Trans. 2* **1993**, 799−805.
(25) Eckert, F.; Klamt, A. *AIChE J.* **2002**, *48*, 369−385.
(26) Bramwell, F. B.; Haddon, R. C.; Wudl, F.; Kaplan, M. L.; Marshall, J. H. *J. Am. Chem. Soc.* **1978**, *100*, 4612−4614.
(27) Blaurock, S. University of Leipzig, Germany. Unpublished results, 2003.
(28) Gillies, J. Z.; Gillies, C. W.; Cotter, E. A.; Block, E.; DeOrazio, R. *J. Mol. Spectrosc.* **1996**, *180*, 139−144.
(29) Fabian, J.; Diaz, L. A.; Seifert, G.; Niehaus, T. *J. Mol. Struct. (THEOCHEM)* **2002**, *594*, 41−53.
(30) Lorance, E. D.; Glass, R. S.; Block, E.; Li, X. *J. Org. Chem.* **2003**, *68*, 8110−8114.